FUDMA Journal of Sciences (FJS)
ISSN online: 2616-1370
ISSN print: 2645 - 2944
Vol. 7 No. 3, June (Special Issue), 2023, pp 223 - 231
DOI: https://doi.org/10.33003/fjs-2023-0703-1863

EVALUATION OF SOLAR ENERGY POTENTIALS FOR POWER ENERGY GENERATION IN MAIDUGURI, BORNO STATE

***Likta, E. W., Gadzama J. K., Malgwi D. I.**

University of Maiduguri, Department of Physics, P.M.B 1069, Maiduguri, Borno State. Nigeria. West Africa.

*Corresponding authors' email: emmalikta2014@gmail.com Phone: +2348057613964

ABSTRACT

Today solar radiation is known as the largest renewable energy that has importance to power generational potential. Also solar radiation is the fundamental component all-natural events and activities in the atmosphere and biosphere. Solar radiation has significance to humanity cannot be overstated because it can be used to generate electricity. Solar energy is an abundant free, clean and it has the potential to provide energy. The goal of this paper is to obtain the solar irradiance potential for Maiduguri and also to obtain the PV power output. Hargreaves Equation is used as the methodological technique for analysis of the data. The solar irradiance potential for Maiduguri has been obtained. The PV power output also has been achieved. Data convention from weather station into radiation on an inclined surface has been observed at an angle of 19˚02'39' N degree latitude. We recommend that the general public should be sensitizing about the benefits of solar energy and also the government should develop a blue print for solar energy generation as soon as possible.

Keywords: Solar, Radiation, Energy, Potential, Power, Irradiance

INTRODUCTION

The primary cause of all natural occurrences and processes in the atmosphere and biosphere is solar radiation. Because it can produce electricity, its importance to humanity cannot be emphasized. In order to use solar energy in a range of applications, it is necessary to understand solar radiation statistics (Zheng et al., 2008). In order to research and develop the economic viability of solar-powered equipment, it is helpful to have a good grasp of a location's global sun radiation. The largest renewable energy source available today is solar radiation, and due to its significance, recent research has focused on how much electricity it can provide. Focus has shifted away from fossil fuels and toward renewable energy sources, such as solar power generation, due to the depletion of fossil fuels and the associated environmental problems (Chineke, 2002).

Nigeria may be able to meet its energy needs for both urban and rural areas because to the plentiful, cost-free, and pure solar energy. On the other hand, fossil fuel-based resources and technology are more long-term than renewable resources. Due to the unpredictability of the country's electrical supply, just 10% of rural families and 40% of the entire population have access to electricity (Wong, 2001). Electricity is scarce throughout the nation. The level of utilization of Nigeria's renewable energy resources needs to be seriously taken into consideration in order to prevent the country from facing an impending energy shortage as the nation works to develop other renewable energies like wind, solar, and biomass to close the generation gap and promote economic growth. Understanding the potential for solar power generation is essential to achieving this goal.

With a focus on global solar data generated between 2020 and 2022, this study assesses the possibility for producing renewable solar energy in Maiduguri and its environs. The study examines the utilization of renewable energy sources, such as solar electricity, to supply Maiduguri with a consistent flow of energy.

MATERIALS AND METHOD

In partnership with the Physics department, data for this study were gathered for three years (2020-2022) from the university weather station. This covers the technique and data collection procedures. This also contains the equations that were applied to the data.

Methodological Approach

The Hargreaves Equation was utilized as the methodological tool for the analysis of the data supplied for this study. This equation is used to quantify global sun radiation for a particular geographic region (Jun et al., 2011). The Hargreaves Equation allows for the calculation of solar radiation R using interplanetary radiation and the difference between the monthly average maximum and minimum air temperature (Chineke, 2002). In graphical profiles, the monthly data fluctuations of the minimum and maximum temperature are displayed, and the profiles' evaluation is considered in the context of the research findings. Design and sizing strategies for freestanding photovoltaic systems, as well as associated economic models, are encouraged in order to analyze their potentials.

Measurement of Solar Radiation

Measurements of solar radiation at various locations across the world are needed to determine the amount of solar energy that is available and reaching the surface of the earth (Chineke, 2002). The two types of solar radiation that reach the earth's surface are direct and diffuse solar radiation (Jun et al., 2011). The direct solar beam, which arrives at the earth's surface directly from the sun without being scattered, reflected, or otherwise dispersed, is the initial part of the system. The latter component is the solar radiation that, as a result of solar beam scattering, reflection, and other dispersion, reaches the earth's surface. To obtain the total (global) solar radiation, the direct and diffuse solar radiation components are summed.

As the sun's energy-bearing particles pass through the atmosphere, some of it is scattered and some is absorbed, weakening the sun's radiation. A variety of equipment with various characteristics and levels of precision can monitor solar radiation. To monitor radiation levels around the world, pyrometers are employed.

Solar Radiation on the Earth Surface

Before solar energy reaches the earth's surface, it must travel through the atmosphere. The amount of radiation that reaches

the earth's surface is influenced by a variety of variables, such as the Earth's distance from the sun, atmospheric influences, declination angle, and others (Jun et al., 2011). The distance between the sun and the earth varies as a result of the elliptical orbit that the earth takes around the solar. When the earth is farthest from the sun, it receives less energy (Augustina, 2009). A component of the solar constant is represented by the actual solar radiation that the earth's surface receives. This is due to the sun's light being partially blocked by the earth's atmosphere. Depending on our distance from the sun and our angle away from it, we also received less solar radiation. Indeed, the sun generates over two billion times as much energy as the Earth does (Escobedo et al., 2009).

Location of the Study Area

In Nigeria, Maiduguri is situated in latitude 11°49'59.99"N and longitude 13°08'60.00"E in the northern region of the country. According to the census taken in 2022, it is 822, 000 people strong and has a total area of 105.5km². The tropical climate in Maiduguri is humid and dry at the same time. The region is characterized by double rainfall maxima. The start of the rainy season in April and its duration through October are subject to annual changes in rainfall.

Data collection and Treatment

Based on the specified climatological parameters, the Hargreaves Equation is used in this study to calculate the global solar radiation for the selected site (Shyam et al., 2011). For information on monthly average maximum and minimum temperatures, solar radiation, and latitude for the years 2020 to 2022, the study relies on data from the Nigerian meteorological station in Maiduguri. According to Hargreaves and the difference between the monthly averages for the highest and lowest air temperatures as well as extraterrestrial radiation can be utilized to calculate Rs (Shyam et al., 2011). The formula for Hargreaves and Samani is as follows:

$R_s = K_f R_a (T_{max} - T_{min}) = 0.5$ (1)

maximum and lowest temperatures (°C), R_a is extra-terrestrial radiation, R_a is global solar radiation, and K_r is the empirical coefficient.

For the interior region, Hargreaves proposed using $k_r = 0.16$. As a result, because Maiduguri is located in the northern region, the K_r value is 0.16. Using the equation below, extraterrestrial radiation (Ra MJm2month^{l}) can be determined.

$R_a = \frac{100}{\pi}$ (GSC.dr) (φ s sin(θ) sin(δ) + cos(δ) sin(φ s)) (2)

Where GSC is the solar constant (0.0820 MJm²month^{1}). dr is the inverse relative distance from earth to sun, φs is the sunset hour angle (rad), φ= latitude (rad), and δ =solar declination (rad). The following formulae can be used to calculate the values

ϕ= arcos (- tanφ tan φ) (3)

$d = 1 + 0.033 \cos\left(\frac{2nJD}{365}\right)$ (4)

δ = 0.409 sin (2rJD - 1.39) (5)

where JD denotes the year's first day.

The bulk of models for predicting the global solar energy potential are based on sunshine hours, sunshine hours, and relative humidity (Augustina, 2009). (Gueynard, 1989). Sun exposure, relative humidity, maximum temperature, latitude, height, and location are all important considerations (Jun et al., 2011). In this study endeavor, it is difficult to employ monthly averages of maximum and lowest temperature, solar radiation, and latitude with sufficient accuracy (Spencer et al., 1982).

RESULTS AND DISCUSSION

Observed and calculated sunshine measurements are among the finest indicators of the amount of solar radiation that is present at a certain location. This chapter provides the monthly average of daily global solar radiation (Hm) in MJ/m2 for the research site Maiduguri, Borno State, for the months of January through December in 2021 and 2022. In order to predict Photo-Active Radiation (PAR) levels over a three-year period (2020, 2021, and 2022), this study employed a site-based technique in which typical metrological data was collected at the study area.

The daily average clearness index (K1) was estimated from the relationship between the hourly total and daily irradiation and the hourly global solar insolation on calculated hourly extraterrestrial horizontal insolation from their respective monthly average daily values. Milliliters were used to measure the GSR data. These were converted to MJm-2 day-1 using the calibration equation:

$1\text{ml} = 1.26 \text{ x } 106\text{jm} - 2 \text{ of Gunn} - \text{Bellani (GB)}$ (6)

Calculated Method of Estimation

The purpose of this research is to apply an empirical model creased to estimate the solar energy potentials accessible in the study area (Maiduguri), and to utilize this model to predict the hourly values of active radiation Q_p.

$\frac{P_s}{Q_p} = 1.832 - 0.191 \lim \text{kt} + 0.099 \sin\alpha$ (7)

(Chow and Wong, 2001) define R_s as the hourly global solar radiation and (degrees) as the solar height, which is related to the zenith angle θ_z by equation 3;

$\text{Sin}\alpha = \cos\theta_z$ (8)

The zenith angle of the Sun is the angle of incidence θ_z;

$\text{Cos}\theta_z = \sin\delta \sin\phi + \cos\delta \cos\phi \cos\omega$ (9)

$\frac{Q_p}{R_s} = 1.832 - 0.191 \lim \text{kt} + 0.099 \sin\alpha$ (10)

As a result, for the model utilized in hourly clearness index is calculated as follows

$K_t = \frac{I}{I_o}$ (11)

Where I is the hourly global sun radiation in Mjm^{-2}hr^{-1} and I_o extraterrestrial solar radiation measured in Mjm^{-2}hr^{-1}, H_0 is determined by the equation;

$H_o = \frac{24}{\pi} I_{sc} E_o \left[\left(\frac{\pi}{180}\right) \omega\text{s}(\sin\delta \sin\phi) + (\cos\delta \cos\phi \cos\omega\text{s})\right]$ (12)

Where I_{sc} = 1367W/m^2 is the Solar Constant, Spenser calculates E_o (dimensionless) as the eccentricity correction factor for the Earth's orbit

$E_o = 1.00011 + 0.034221\cos\Gamma' + 0.000719\cos 2\Gamma' + 0.000077\sin 2\Gamma'$ (13)

The equation can be used to compute extraterrestrial hourly in Mjm^{-2}hr^{-1}

$I_o = I_{sc} E_o (\sin\delta \sin\phi + 0.9972 \cos\delta \cos\phi \cos\omega 1)$ (14)

Where I_{sc} denoted the solar constant in Mjm^{-2}hr^{-1}, declination, latitude and hour angle are all measured in degrees at the middle of an hour. The day's perspective Γ'

$\Gamma' = 2(\text{N-}136)$ (15)

$\Gamma'_1 = \frac{\pi}{2}(\cos\omega \text{I})$ (16)

in the middle of the hour, the hour angle is measured in degrees.

Data Presentation

The average hourly values of PAR (Q_p), which are derived from average hourly global solar radiation, were calculated using the second k_t model in equation 10 to arrive at the values of Q_p presented in table 2. The tables show almost identical seasonal variance for the months of January 2020, 2021, and 2022, with the hourly Q_p peaking daily at 12pm. The hour

angle s, the extraterrestrial monthly horizontal worldwide sun irradiation Ho, and the hourly global solar radiation 10, r_t (which is the ratio of the hourly total to day irradiation), are all crucial factors (hourly PAR) for figuring out Q_p.

Tables 2 and 3 show the results of the computations for the hourly clearness index kt and the cosine of the zenith angle cosz. With respect to local time, these statistics demonstrate seasonal variation. Figure 2 demonstrates the comparable trend between Qp and Rs. The table also includes the anticipated values for the mean hourly PAR and Qp for 2020, 2021, and 2022.

Table 1: Estimated Hourly PAR to hourly Global Radiation Ratios for the months of January, February and March in 2020, 2021 and 2022

Local Time	S 2020 (µEJ)				S 2021 (µEJ)				S 2022 (µEJ)			
	Jan	Feb	Mar	Apr	Jan	Feb	Mar	Apr	Jan	Feb	Mar	Apr
7:00am	1.94	1.92	1.94	1.95	1.90	1.92	1.94	1.95	1.98	1.94	1.97	1.89
8:00am	1.96	1.94	1.96	1.97	1.92	1.95	1.96	1.95	2.09	1.96	1.99	1.99
9:00am	1.97	1.96	1.98	1.95	1.94	1.96	1.98	1.96	2.03	1.98	2.01	1.95
10:00am	1.99	1.97	1.99	1.96	1.95	1.98	1.99	1.97	2.04	1.99	2.03	1.97
11:00am	2.02	1.98	2.09	1.97	1.96	1.99	2.01	1.98	2.05	1.99	2.04	1.98
12:00pm	2.05	1.99	2.01	1.98	1.96	1.99	2.01	1.99	2.05	2.09	2.04	1.99
1:00pm	2.02	1.98	2.09	1.97	1.96	1.99	2.09	1.98	2.05	1.99	2.03	1.98
2:00pm	1.99	1.97	1.99	1.96	1.95	1.98	1.99	1.97	2.04	1.99	2.03	1.98
3:00pm	1.97	1.96	1.98	1.95	1.94	1.96	1.98	1.96	2.03	1.98	2.01	1.95
4:00pm	1.96	1.94	1.96	1.97	1.92	1.94	1.96	1.95	2.09	1.96	1.99	1.99
5:00pm	1.94	1.92	1.16	1.95	1.90	1.92	1.94	1.95	1.97	1.94	1.97	1.89

Table 2: Hourly Par to Hourly Global Radiation Ratio Estimated Values June, July, August and September of 2020, 2021 and 2022

Local	Q_p/R_s 2020 (µEJ^{-1})				Q_p/R_s 2021 (µEJ^{-1})				Q_p/R_s 2022(µEJ^{-1})			
Time	May	Jun	Jul	Aug	May	Jun	Jul	Aug	May	Jun	Jul	Aug
7:00am	2.05	2.02	2.02	2.02	2.11	2.02	1.99	2.02	2.02	2.03	2.09	2.10
8:00am	2.05	2.03	2.04	2.04	2.11	2.03	2.01	2.05	2.03	2.04	2.11	2.13
9:00am	2.06	2.04	2.06	2.06	2.12	2.04	2.03	2.06	2.06	2.05	2.13	2.15
10:00am	2.06	2.06	2.07	2.07	2.02	2.06	2.05	2.08	2.06	2.05	2.15	2.16
11:00am	2.06	2.08	2.08	2.08	2.02	2.08	2.05	2.09	2.06	2.06	2.15	2.17
12:00pm	2.06	2.09	2.08	2.08	2.02	2.09	2.06	2.09	2.06	2.07	2.16	2.17
1:00pm	2.07	2.09	2.08	2.08	2.02	2.09	2.05	2.09	2.06	2.07	2.15	2.17
2:00pm	2.07	2.06	2.07	2.07	2.02	2.06	2.05	2.08	2.06	2.06	2.15	2.16
3:00pm	2.06	2.05	2.06	2.06	2.02	2.05	2.03	2.06	2.06	2.05	2.13	2.15
4:00pm	2.07	2.03	2.04	2.04	2.02	2.03	2.01	2.05	2.03	2.04	2.11	2.13
5:00pm	2.05	2.02	2.02	2.02	2.12	2.02	1.99	2.03	2.02	2.03	2.09	2.10

Table 3: Hourly Par to Hourly Global Radiation Ratio Estimated Values for September, October, November and December of 2020, 2021 and 2022

Local Time	Q_p/R_s 2020 (µEJ^{-1})				Q_p/R_s 2021 (µEJ^{-1})				Q_p/R_s 2022 (µEJ^{-1})			
Time	Se*p	Oct	Nov	Dec	Sep	Oct	Nov	Dec	Sep	Oct	Nov	Dec
7:00am	1.98	2.08	1.90	1.96	1.97	1.21	1.92	1.96	2.04	1.11	1.92	1.96
8:00am	2.01	2.01	1.92	1.96	1.99	1.22	1.95	1.96	2.06	1.20	1.95	1.96
9:00am	2.02	2.02	1.92	1.97	2.02	1.02	1.96	1.98	2.08	2.02	1.96	1.98
10:00am	2.04	2.05	1.94	1.99	2.03	2.04	1.98	1.99	2.10	2.04	1.98	1.99
11:00am	2.05	2.05	1.95	1.02	2.04	2.05	1.98	1.02	2.11	2.05	1.98	1.00
12:00pm	2.05	2.05	1.95	2.05	2.05	2.05	1.99	1.05	2.10	2.05	1.99	1.00
1:00pm	2.05	2.05	1.95	1.02	2.04	2.05	1.98	1.02	2.11	2.05	1.98	1.02
2:00pm	2.04	2.04	1.95	1.99	2.04	2.04	1.98	1.99	2.10	2.04	1.98	1.99
3:00pm	2.02	2.02	1.92	1.97	2.02	1.02	1.96	1.97	2.08	2.02	1.96	1.96
4:00pm	2.01	2.01	1.92	1.96	2.06	1.21	1.95	1.96	2.06	1.20	1.95	1.96
5:00pm	1.98	1.98	1.90	1.96	1.97	1.21	1.92	1.94	2.04	1.11	1.92	1.94

According to the hourly pattern of the ratio of active photon density flux to broadband solar irradiance hourly values for all the months in the years 2020, 2021, and 2022, Table 1─3 displays the hourly ratio of active photon density flux to broadband solar irradiance values for all months in the years 2020, 2021, and 2023. Tables 1–3 also include the local time for the dry and wet seasons. The biggest value of these variations in the hourly Qp/Rs 2022 (EJ-1) for the years is identified around lunchtime. The table also shows that these ratios show greater seasonal and daily changes during the wet season than they do during the dry season. Due to these tables, the ratio is larger and more unpredictable during the rainy season than it is during the dry season, and it is typically higher at noon.

Table 4: Estimated Hourly Par Values for the Month of January 2020

Local Time	I_o Mjm2hr^{-1}	Cosθz	H_o Mjm^{-2}	r_t	H_m Mjm^{-2}	I Mjm2hr^{-1}	K_r	Q_p (2020)
7:00am	0.89	0.17	32.0	0.02	20.2	0.43	0.47	0.84
8:00am	2.02	0.39	32.0	0.05	20.2	1.09	0.54	2.17
9:00am	2.89	0.58	32.0	0.08	20.2	1.79	0.60	3.57
10:00am	3.72	0.73	32.0	0.12	20.2	2.40	0.65	4.78
11:00am	4.18	0.83	32.0	0.14	20.2	2.83	0.76	5.62
12:00pm	4.35	0.85	32.0	0.14	20.2	2.97	0.68	5.91
1:00pm	4.18	0.83	32.0	0.15	20.2	2.83	0.67	5.62
2:00pm	3.72	0.734	32.0	0.12	20.2	2.40	0.65	4.78
3:00pm	2.89	0.58	32.0	0.09	20.2	1.79	0.60	3.56
4:00pm	2.02	0.39	32.0	0.05	20.2	1.09	0.54	2.17
5:00pm	0.89	0.17	32.0	0.02	20.2	0.43	0.47	0.84

Table 5: Estimated Hourly PAR values for the Month of January 2021

Local Time	I_o Mjm2hr^{-1}	Cosθz	H_o Mjm^{-2}	r_t	H_m Mjm^{-2}	I Mjm2hr^{-1}	K_r	Q_p (2021)
8:00am	2.02	0.39	32.0	0.05	24.8	1.34	0.66	2.61
9:00am	2.89	0.58	32.0	0.08	24.8	2.20	0.74	4.30
10:00am	3.72	0.74	32.0	0.12	24.8	2.95	0.79	4.75
11:00am	4.18	0.83	32.0	0.14	24.8	3.47	0.83	6.77
12:00pm	4.34	0.86	32.0	0.14	24.8	3.65	0.84	7.11
1:00pm	4.18	0.83	32.0	0.15	24.8	3.47	0.83	6.76
2:00pm	3.72	0.73	32.0	0.12	24.8	2.95	0.79	5.75
3:00pm	2.89	0.58	32.0	0.08	24.8	2.21	0.74	4.30
4:00pm	2.02	0.39	32.0	0.05	24.8	1.34	0.66	2.61
5:00pm	0.89	0.17	32.0	0.02	24.8	0.52	0.58	1.02

Table 6: Estimated Hourly PAR values for the Month of January 2022

Local Time	I_o Mjm2hr^{-1}	Cos^{2}hr^{-1}	$H_o\theta$z	r_t Mjm^{-}	H_m Mjm^{-}	I Mjm^{-1}	K_r(2022)θz	Q_p
8:00am	2.02	0.39	32.0	0.05	24.8	1.34	0.42	1.72
9:00am	2.89	0.58	32.0	0.08	24.8	2.20	0.46	2.83
10:00am	3.72	0.73	32.0	0.12	24.8	2.95	0.49	3.78
11:00am	4.18	0.83	32.0	0.14	24.8	3.47	0.42	4.45
12:00pm	4.35	0.85	32.0	0.14	24.8	3.65	0.53	4.67
1:00pm	4.18	0.83	32.0	0.15	24.8	3.47	0.42	4.45
2:00pm	3.72	0.73	32.0	0.12	24.8	2.95	0.49	3.78
3:00pm	2.89	0.58	32.0	0.08	24.8	2.21	0.46	2.28
4:00pm	2.02	0.39	32.0	0.05	24.8	1.34	0.42	2.72
5:00pm	0.89	0.17	32.0	0.02	24.8	0.52	0.36	1.67

The hourly global solar radiation, I, the hourly horizontal extraterrestrial global radiation, Io, the hour angle, s, the extraterrestrial monthly horizontal global solar irradiation, H_o, and the hourly clearness index, k_t are among the calculated parameters adopted for the model used in this study. R_t is the ratio of the hourly total to daily irradiation. These figures show seasonal variance in relation to the local time. Table demonstrates that Q_p and R_s have a comparable trend.

Table 7: Estimated Average Hourly PAR to Hourly Global Radiation Ratios and Average Hourly PAR, Q_p, for 2020, 2021 and 2022

Months			N	ω/^{o}	δ	H_o	I$^{'}$	E_o	Q_p(EMJ^{-})		
			Q_p(EMJ^{-})		Q_p(EMJ	MJm^{-2})^2)^2)			2020		
						2021			2022		
Jan	15	86.12	-21.15		33.00	13.81	1.04	3.56	4.364	2.87	
Feb	45	87.71	-12.90		34.70	44.38	1.03	4.28	4.090	3.99	
Mar	73	89.56	-2.42		37.00	72.00	1.01	4.17	4.303	3.73	
Apr	105	91.72	9.78		37.90	102.28	0.90	2.22	4.262	3.62	
May	135	93.67	19.03		37.50	134.16	0.97	4.04	3.177	2.77	
Jun	166	94.43	23.35		37.10	162.10	0.97	3.17	3.604	2.66	
Jul	196	93.88	21.07		37.20	192.30	0.96	2.90	3.452	2.14	
Aug	227	92.40	13.45		36.00	223.00	0.97	2.96	2.789	1.95	
Sep	258	90.32	1.98		37.00	254.44	0.99	3.58	3.663	2.74	
Oct	288	88.23	-9.97		35.00	283.01	1.01	2.89	3.946	3.54	
Nov	319	86.46	-19.38		32.40	313.64	1.02	3.82	4.020	3.58	
Dec	360	85.65	-23.40		31.00	344.33	1.034	3.75	4.082	3.54	

Table 8: Hourly PAR, Q_p Average Estimated Values for January, June, August and June of 2020, 2021 and 2022

Local time	Q_p(January) $MJm^{-2}h^{-1}$	Q_p(June) $MJm^{-2}h^{-1}$	Q_p(August) $MJm^{-2}h^{-1}$	Q_p(August) $MJm^{-2}h^{-1}$
7:00am	0.84	0.76	0.63	0.91
8:00am	2.16	1.92	1.37	2.34
9:00am	3.56	3.13	2.59	3.85
10:00am	4.77	4.17	3.46	5.12
11:00am	5.61	4.89	4.06	6.09
12:00pm	5.89	5.14	4.27	6.37
1:00pm	5.61	4.89	4.06	6.09
2:00pm	4.77	4.17	3.45	5.15
3:00pm	3.56	3.13	2.59	3.85
4:00pm	2.16	1.92	1.37	2.34
5:00pm	0.84	0.76	0.76	0.63

The expected mean hourly PAR and Qp values for 2020, 2021, and 2022 are shown in Table 7. The table demonstrates that the Qp values are higher during the dry season and lower during the rainy season. A more detailed variation of the anticipated Qp across 2020, 2021, and 2022 is also shown in Table 8. The months of the dry season are January and December, whereas the months of the wet season are June and August.

This further illustrates that hourly values are higher in dry season months than in wet season months. The highest Qp, however, was attained at midday on all seasons at roughly 12 p.m.

Table 9: Estimated Hourly PAR to hourly Global Radiation Ratios for the months of January to December in 2020, 2021 and 2022

Months	2020	2021	2022
January	3.50	7.90	10.80
February	4.15	8.15	12.15
March	4.10	8.30	12.10
April	3.00	7.50	11.00
May	4.00	7.45	10.00
June	3.00	6.90	9.50
July	2.50	6.30	8.50
August	2.50	6.30	8.50
September	3.80	7.50	10.00
October	2.50	7.00	10.20
November	3.90	7.90	11.50
December	3.90	7.90	11.50

Table 10: Hourly Par to Hourly Global Radiation Ratio Estimated Values January to December 2020, 2021 and 2022

S/N	Local Time	2020	2021	2022
1	7:00am	1.00	2.00	2.20
2	8:00am	2.10	4.50	6.50
3	9:00am	3.80	8.00	10.50
4	10:00am	5.00	10.50	14.50
5	11:00am	5.90	12.50	17.00
6	12:00pm	6.00	13.00	17.85
7	1:00pm	5.90	12.50	17.00
8	2:00pm	5.00	10.50	14.50
9	3:00pm	3.80	8.00	10.50
10	4:00pm	2.10	4.50	6.50
11	5:00pm	1.00	2.00	2.20

Table 11: Hourly Par to Hourly Global Radiation Ratio Estimated Values for January to December 2020, 2021 and 2022

S/N	GMT	I	I_o
1	7:00am	0.48	0.96
2	8:00am	1.20	2.00
3	9:00am	1.86	3.00
4	10:00am	2.48	3.80
5	11:00am	2.89	4.20
6	12:00pm	3.00	4.20
7	1:00pm	2.89	4.20

8	2:00pm	2.48	3.80
9	3:00pm	1.86	3.00
10	4:00pm	1.20	2.00
11	5:00pm	0.48	0.96

Table 12: Estimated Hourly Par Values for the Month of January to December 2020, 2021 and 2022

S/N	Month	H	H_o
1	January	25.00	33.00
2	February	24.50	35.00
3	March	24.70	36.00
4	April	24.00	38.00
5	May	17.5	38.00
6	June	20.00	36.00
7	July	19.00	36.00
8	August	15.10	35.50
9	September	20.00	35.65
10	October	22.60	35.00
11	November	23.50	33.00
12	December	24.80	31.00

Results Analysis

The tables show that the mean hourly Q_p/R_s(EJ-1) for the dry season months is 1.900, whereas the mean hourly $Q_p/R_s(EJ^{-1})$ for the rainy season months is 2.000. The tables also display the yearly distribution of the daily monthly means of the ratio of active radiation to solar irradiation. As a result, crucial plots that were necessary for effective interpretation were made in order to clearly analyze the outcomes.

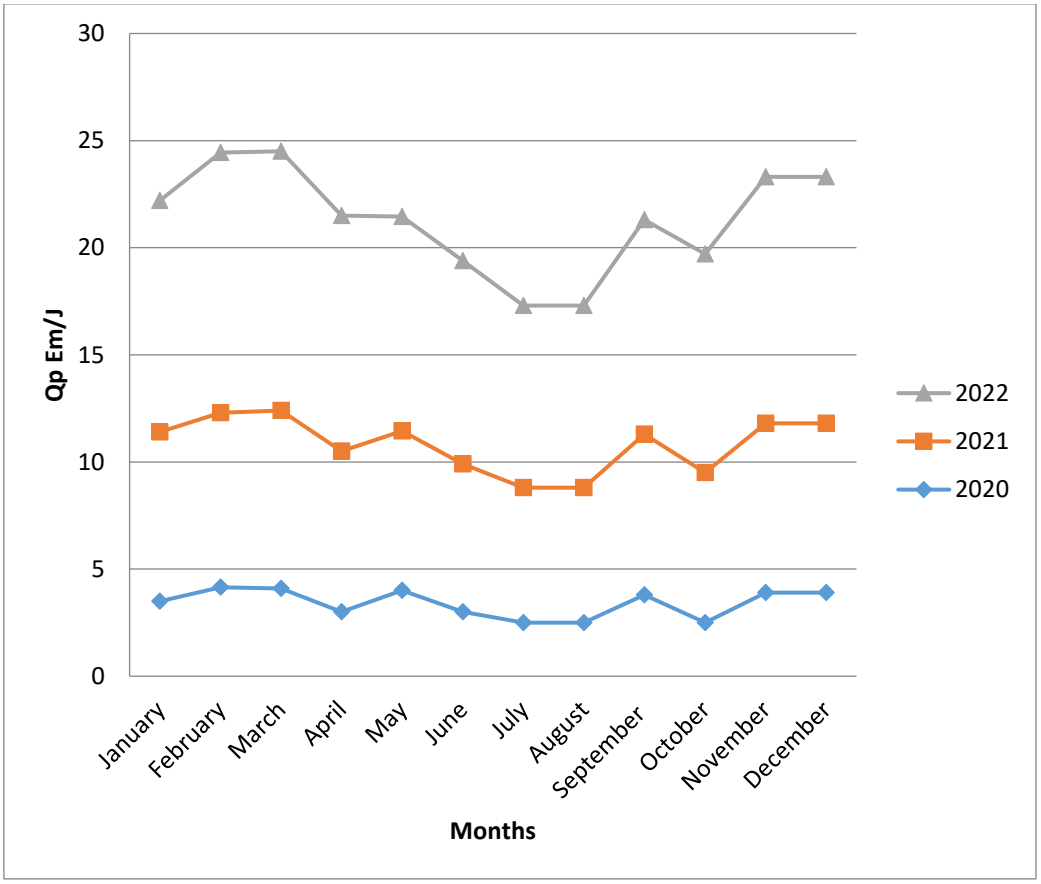

Figure 1: Variation of Average Monthly PAR (Q_p) for 2020, 2021 and 2022

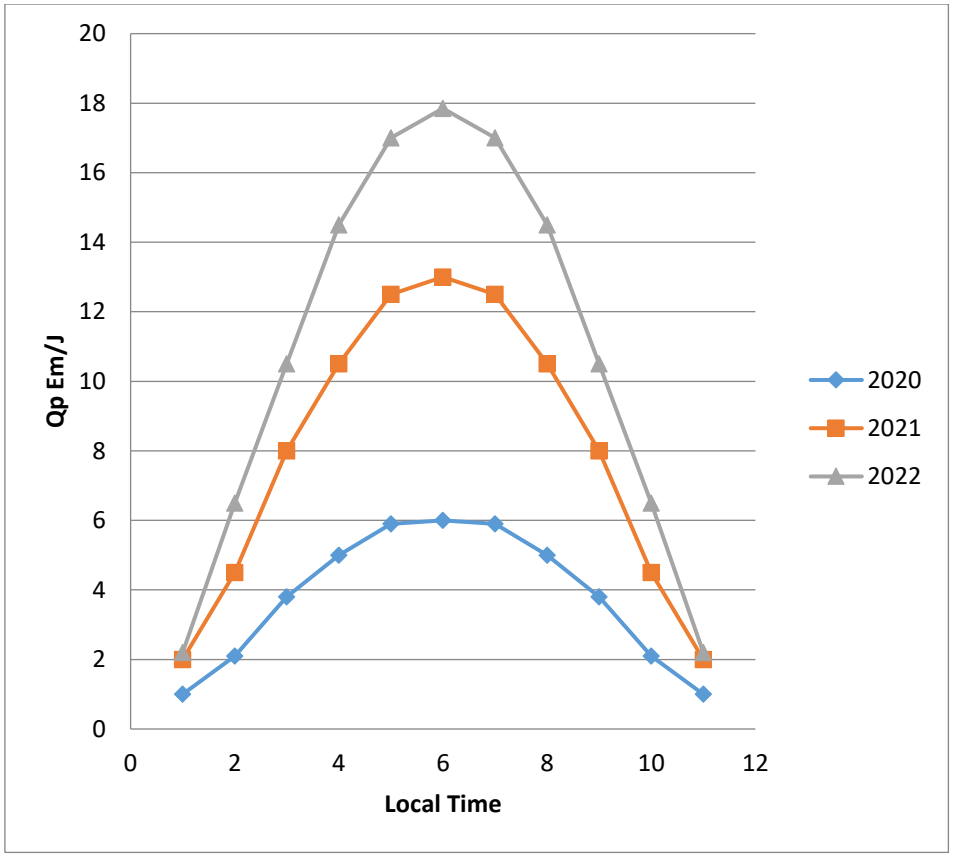

Figure 2: Variation of Hourly PAR with Local Time for January of 2020, 2021 and 2022

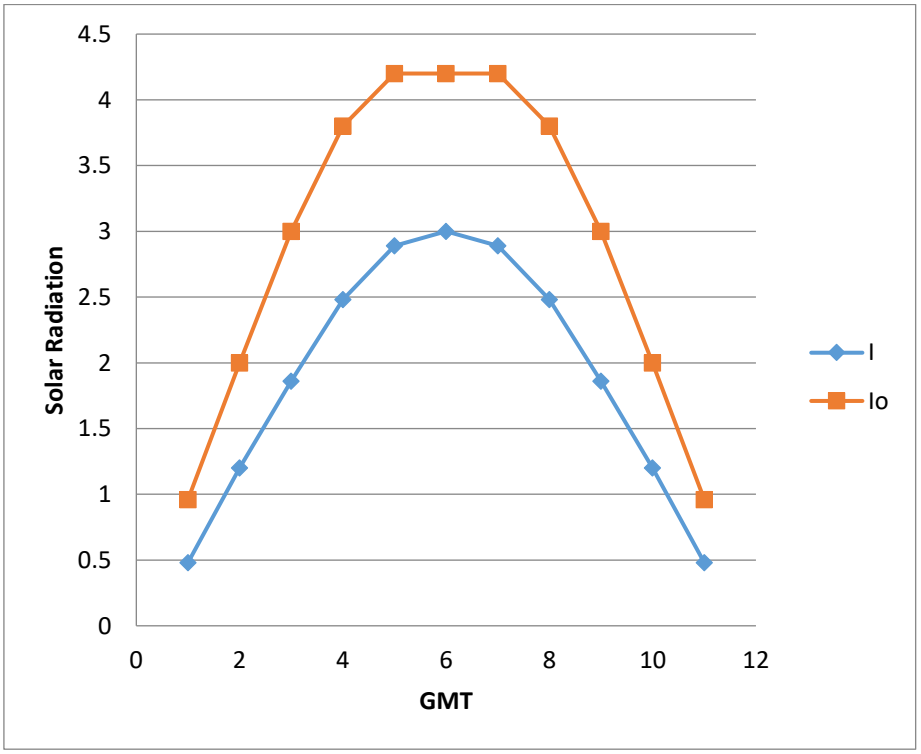

Figure 3: The Monthly Variation of Global extraterrestrial solar radiation, I_o

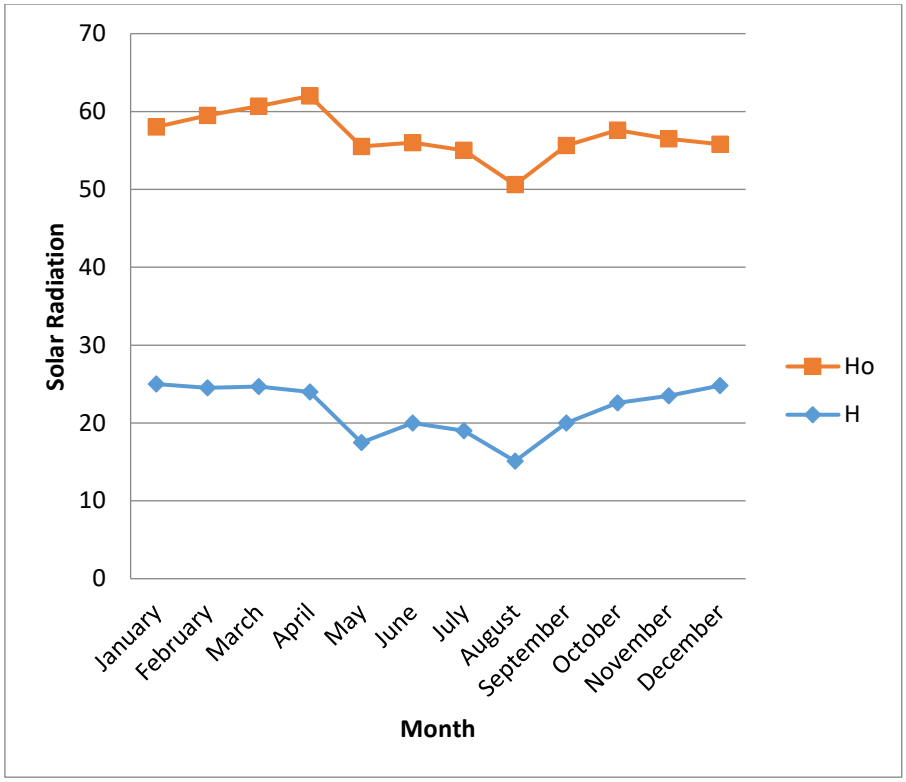

Figure 4: The monthly variation of global extraterrestrial solar radiation, H_o

Discussion

Solar radiation, sometimes referred to as Photo Active Radiation (PAR), is the quantity of light with a wavelength accessible for photosynthesis that has a range from 400 to 700 manometers. Figure 1 shows that the three years that is 2020, 2021 and 2022 are having a slit zigzag line which indicates that 2022 is having the highest Average monthly variation followed by 2021 and then 2020. In general, for the three years it proves that the month of February and March are having the highest Average Monthly variation followed by September, November and December while the Month of July and August are the lowest Average Monthly variation. Figure 2 indicates the three years Hourly variation for Local time in the Month of January 2020, 2021 and 2022. The figure looks like a curve which shows that at the 6 hour of the Local time is having the highest Q_p EmJ^{-1} for the three years followed by 5 hour and 6 hour while the lowest are 1 hour and 11 hour. Figure 3 proves that the month variation of Global extraterrestrial solar radiation is like a curve shape. It indicates that the 5 hour and 7 hour at GMT of the Global extraterrestrial (I_o) are on the same level of solar radiation while for total extraterrestrial (I) at 6 hour GMT is having the highest solar radiation. In general, 1 hour GMT and 11 hour GMT are having the lowest solar radiation. Figure 4 shows that the monthly variation Global extraterrestrial solar radiation is like a shape of 'w'. The Global extraterrestrial solar radiation H_o indicates that the month of April is having the highest solar radiation while for the month of August is having the lowest solar radiation. The total extraterrestrial solar radiation H proves that the month of January and December are having the highest solar radiation while the month of August is having the lowest solar radiation. In general, the month of May and August are having the lowest solar radiations.

Generally in figure 1 to 4, the fluctuates are according to the season, latitude, and hour of the day. In comparison to the months of the dry and harmattan seasons, the months of the wet and rainy seasons have a lower Q_p. The Q_p for June, July, and August in 2022 was 3.176 EmJ^{-1}, 2.900 EmJ^{-1}, and 2.960 EmJ^{-1}, respectively. The same year's November, December, and January each show temperatures of 3.871EmJ^{-1}, 3.997EmJ^{-1}, and 3.655EmJ^{-1}. These statistics show that the Q_p is higher throughout the entire dry season of the year. This may be caused by the clear sky and sparse cloud cover.

According to Tables 4, 5, and 6, the months of December an d January in the harmattan have lower Q_p values than other d ry season months because of the high concentrations of dust from the harmattan and the high levels of scattering aerosols in the air caused by bush burning.

According to these tables, the mean hourly Qp/Rs(EJ-1) for the dry season months is 1.900, while the mean hourly Qp/Rs(EJ-1) for the rainy season months is 2.000. Additionally, the tables display the daily and monthly means of the Qp/Rs ratio, which denotes the ratio of photo synthetically active radiation to broadband solar irradiance and may be seasonal. The monthly variation of the total amount of extraterrestrial solar radiation, H. This is so that atmospheric factors cannot affect extraterrestrial horizontal insolation per day estimated at a certain location, which is insolation on a horizontal surface. Extraterrestrial horizontal insolation is simply a function of latitude and the day of the year, as shown by equation 12.

According to Wong, the clearness index, k_t, gives a measure of the atmospheric effects at a location on the insolation, which is a measure of the climatic state at a geographical location.

CONCLUSION

The seasonal relation of the ratio of photo synthetically active radiation to broadband solar radiation was discovered by analysis of data on photo synthetically active radiation and broadband solar radiation collected in Maiduguri, north-east

Nigeria, from January 2020 to December 2022. The dry season has lower and more erratic numbers, whereas the wet season has greater figures. The dry season months of December, January, February, March, and April had the highest values, while the wet season months of June, July, August, September, and October saw the lowest values, according to the hourly values of Q_p for this time. However, the hourly trend of the ratio of broadband solar irradiance to synthetically-active photon density flux (Q_p/R_s) for all seasons shows higher values around noon.

However, the results of this study show that solar radiation is more prevalent in Maiduguri, where solar energy systems may run effectively all year long. As a result, the research region offers a great potential for solar radiation on a worldwide scale and exciting potential for solar energy use.

REFERENCES

Augustine, C., Nnabuchi M.N. (2009). Relationship between global solar radiation and sunshine hours for Calabar, Port Harcourt and Enugu, Nigeria. International Journal of Physical. Sciences. Vol: 4(4):182-188.

Chineke, T.C. (2002). Robust method of evaluating the solar energy potential of a data sparse site. The physical scientist. Vol;1(1):59–69.

Escobedo J. F. Gomes E.N, Oliveira A. P, and Soares J. (2009). "Modelling hourly and daily fractions of UV, PAR and NIR to global solar radiation under various sky conditions at Botucatu, Brazil," Appl. Energy., vol. 86, pp. 299-309.

Gueynard C. (1989). "A two- band model for the calculation of illuminance and photosynthetically active radiation at the earth's surface," Solar Energy, vol. 43, pp. 253-265.

Jun Q., Kun Y. Shunlin L, and Wenjun T. (2011). "Estimation of daily mean photosynthetically active radiation under all-sky conditions based on relative sunshine data," Journal of Applied Meteorology and Climatology, vol. 51, pp. 150-160.

Shyam S, ChandelR, and Aggarwal K. (2011). "Estimation of hourly solar radiation on horizontal and inclined surfaces in Western Himalayas,"Smart Grid and Renewable Energy, vol. 2, pp. 45-55.

Spencer J. (1982). "A comparison of methods for estimating hourly diffuse solar-radiation from global solar-radiation," Solar Energy, vol. 29, Pp. 19-32.

Wong L. T and W. K. Chow (2001). "Solar radiation model," Applied Energy, vol. 69, pp. 191-224.

Zheng T, Liang S, and Wang K. (2008). "Estimation of incident photosynthetically active radiation from GOES visible imagery,"Appl J. Meteor. Climatol., vol. 47, pp. 853-868.